

RAPID COMMUNICATION

Magnetic-Field-Induced Step-like Transitions in Mn-Site Doped Manganites

S. Hébert, V. Hardy, A. Maignan, R. Mahendiran, M. Hervieu, C. Martin, and B. Raveau¹*Laboratoire CRISMAT, UMR 6508 associée au CNRS, ISMRA 6 Boulevard du Maréchal Juin, 14050 Caen, Cedex, France*

Received January 2, 2002; in revised form January 16, 2002; accepted January 25, 2002

An experimental study of the low T magnetic field dependence of the magnetization, specific heat and resistivity for an orbital and charge-ordered perovskite manganite doped in the Mn-site is presented. Well-defined steps are found in all these three physical properties. The abruptness of these jumps for $T < 10$ K suggests some similarities to the Barkhausen effect and to the martensitic transition. This is a new illustration of the rich physics related to the phase separation. © 2002 Elsevier Science (USA)

Due to the richness of their physics (1), the perovskite manganites of formula $\text{Ln}_{1-x}\text{Ae}_x\text{MnO}_3$, where Ln and Ae are a trivalent lanthanide and a divalent alkaline-earth cations, respectively, have been the focus of intensive research these last years. Earlier it was proposed by Zener that the double-exchange (DE) model can explain the simultaneous paramagnetic (PM) to ferromagnetic (FM) and insulator (I) to metal (M) transitions occurring at T_C in these Mn^{3+} ($t_{2g}^3 e_g^1$)/ Mn^{4+} ($t_{2g}^3 e_g^0$) based 3D structures (2).

However, this DE model cannot explain alone the colossal magnetoresistance (CMR) observed for these oxides, which exhibit resistivity drops by several orders of magnitude as shown for Sr- or La-doped $\text{Pr}_{0.7}\text{Ca}_{0.3}\text{MnO}_3$ (3, 4). In fact for the $\text{Ln}_{0.7}\text{Ae}_{0.3}\text{MnO}_3$ manganites, below a critical size of the A site cation, charge and orbital ordering appears, and phase separation phenomena are observed when cooling the samples from room temperature. This is the case of $\text{Pr}_{0.7}\text{Ca}_{0.3}\text{MnO}_3$ whose single-phase paramagnetic insulating state (PMI) is progressively transformed into a mixture of two phases coexisting at the microscopic scale (10–100 nm), an insulating orbitally charge-ordered (OO–CO) phase, and a ferromagnetic metallic (FMM) phase (5, 6). The OO/CO phenomena in these manganites

are thought to be the result of the tendency of their Jahn–Teller Mn^{3+} cations to separate in the form of alternating Mn^{3+} and Mn^{4+} stripes, for which the ordered d_z^2 orbitals are rotated by 90° in two successive Mn^{3+} planes (7). The Jahn–Teller nature of Mn^{3+} species is thus responsible for the strong coupling between charge, spin and the lattice in these materials (8). In the phase-separated state, the $\text{Pr}_{0.7}\text{Ca}_{0.3}\text{MnO}_3$ insulator is amenable to a metallic state by different external sources [electron irradiation, X ray, pressure, magnetic field, electrical field (6, 9–11)] and its high sensibility to several kinds of perturbations is understood as a partial melting of the OO/CO insulating regions into FMM ones which allows to cross the percolation threshold (from I to M) to yield CMR properties.

In the case of the $\text{Ln}_{0.5}\text{Ca}_{0.5}\text{MnO}_3$ manganites, the OO/CO state which corresponds to the 1:1 ratio of $\text{Mn}^{3+}:\text{Mn}^{4+}$ stripes is much more stable as shown for $\text{Pr}_{0.5}\text{Ca}_{0.5}\text{MnO}_3$ which remains insulator without any significant CMR signature up to 27 T (12). Nevertheless, substitutions at Mn site, especially with magnetic cations such as cobalt, chromium, nickel, ruthenium, rhodium and iridium have shown to be very efficient in destroying or weakening the CO/OO state and to allow the development of a ferromagnetic metallic (FMM) state (13–18). The so-doped manganites were found to exhibit a great analogy with relaxor ferroelectrics, as shown for $\text{Nd}_{0.5}\text{Ca}_{0.5}\text{Mn}_{1-x}\text{Cr}_x\text{O}_3$ whose relaxor ferromagnetic behavior is explained by the existence of a quenched random field originating from the Cr impurities (19). Among their peculiarities, these doped manganites show aging and magnetic field annealing effects (19) and also a spectacular increase of the resistivity upon thermal cycling (20). Bearing in mind the great sensitivity to external perturbations of the OO/CO state of these doped manganites, we have revisited the $\text{Pr}_{0.5}\text{Ca}_{0.5}\text{MnO}_3$ oxide doped with 5% Ga and 3% Mg, which are at the boundary between ordering and disordering of charges and orbitals. In this

¹To whom correspondence should be addressed. Fax : 33 2 31 95 16 00. E-mail: bernard.raveau@ismra.fr.

rapid communication, we evidence for these materials a series of step-like transitions at low temperature ($T < 10$ K) in the magnetic field dependence of the specific heat, magnetization and resistivity. From the experimental point of view, this behavior is close to the magnetization avalanches found at the AFM–FM (saturated paramagnetism “PM”) phase transition in $\text{Fe}_x\text{Mg}_{1-x}\text{Cl}_2$ (21) which is sensitive to the impurity.

The $\text{Pr}_{0.5}\text{Ca}_{0.5}\text{Mn}_{1-x}\text{M}_x\text{O}_3$ ceramic samples were prepared by conventional solid-state reaction. Stoichiometric mixtures of the oxides Pr_6O_{11} , CaO , MnO_2 and MO_x ($M = \text{Ga}^{3+}$, Mg^{2+} , Ru^{4+} , Cr^{3+}) were intimately ground and the powders, first heated at 1000°C , were pressed in the form of bars (typical dimensions $2 \times 2 \times 10$ mm). The sintering was made at 1200°C and at 1500°C for 12 h and the bars were then slowly cooled down to 800°C ($5^\circ\text{C}/\text{h}$) and finally quenched to room temperature. The purity of the so-prepared polycrystalline samples was checked by X-ray powder diffraction and by electron microscopy (electron diffraction “ED” and EDS) and also from powder neutron diffraction for the pristine and the Cr-doped manganites (13). At RT, all samples were found to crystallize in the $Pnma$ orthorhombic space group ($a \sim c \sim a_p\sqrt{2} \sim 5.4 \text{ \AA}$ and $b \sim 2a_p \sim 7.6 \text{ \AA}$, where a_p is the primitive cell parameter) and, in the accuracy of the technique, the EDS cationic analyses revealed a good agreement with nominal compositions. The physical properties were measured by using a physical properties measurements system (four-probe resistivity and specific heat) and an ac–dc SQUID magnetometer (magnetization and ac-magnetic susceptibility), both systems from Quantum Design company. For each technique, a different piece of sample from the same batch has been used. Between two successive runs of measurement at low temperature as a function of the magnetic field, the sample was thermally cycled under no magnetic field up to 300 K and down to the measurement temperature. After such zero-field-cooling process from room temperature, the field increasing collection of data up to the maximum field will systematically be referred to as a “virgin curve” even if it is not the first series of measurements for that sample.

The T -dependent ac magnetic susceptibility of these doped manganites is significantly different from the pristine phase $\text{Pr}_{0.5}\text{Ca}_{0.5}\text{MnO}_3$ (Fig. 1). The latter indeed shows a large drop of χ' below $T_{\text{CO}} = 250$ K whereas only a small bump is observed for the Ga-doped oxide. Furthermore, a clear cusp is induced in the 5% Ga-doped phase at $T_g \approx 50$ K. Such cusps are generally observed in spin glasses, so that T_g represents here the freezing temperature. Such a different magnetic behavior of the Ga-doped manganite with respect to the pristine phase is easily explained by the impurity disorder effect which hinders the long-range ordering of charge and orbitals. The electron diffraction study of this doped manganite registered at 92 K confirms

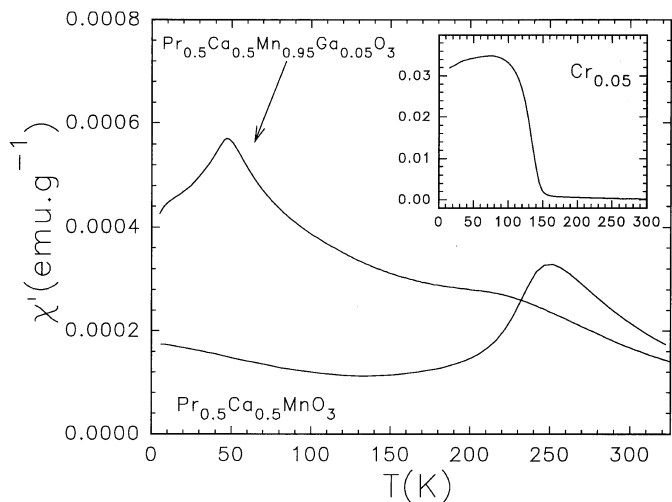


FIG. 1. T -dependent ac-magnetic susceptibility (real part) for $\text{Pr}_{0.5}\text{Ca}_{0.5}\text{Mn}_{0.95}\text{Ga}_{0.05}\text{O}_3$ and for $\text{Pr}_{0.5}\text{Ca}_{0.5}\text{MnO}_3$ ($h_{\text{ac}} = 10$ Oe; $h_{\text{dc}} = 0$ Oe; $f = 1$ kHz). Inset: same curve for $\text{Pr}_{0.5}\text{Ca}_{0.5}\text{Mn}_{0.95}\text{Cr}_{0.05}\text{O}_3$.

the coexistence of regions with or without an incommensurate modulated phase. When the satellites are observed, the modulation vector (qa^*) is parallel to the $[100]^*$ direction with slightly different q values (average $q \approx 0.4$). The selected area electron diffraction (SAED) study showed that the sharpness and intensity of the satellites vary depending on the crystal zones. This is illustrated by two $[010]$ ED patterns, recorded in two adjacent regions of the same crystallite. In Fig. 2a, the satellites are weak but clearly visible whereas they can hardly be observed in Fig. 2b. The broadness and the varying intensity of these extra peaks are consistent with the lattice images recorded at 92 K with a Jeol 2010 electron microscope (Fig. 2c). They exhibit systems of fringes which are not perfectly parallel and regularly spaced as in $\text{Pr}_{0.5}\text{Ca}_{0.5}\text{MnO}_3$. They are characterized by a high density of dislocation like defects (seen at grazing incidence) showing that the OO/CO structure is highly disturbed. Moreover, in the crystal regions with no or only weak satellites in the ED patterns, the lattice images show the presence of $Pnma$ -type structure, i.e., no OO/CO ordering over regions extending from a few to a thousand nanometers width. This is a direct evidence of a phase separation at 92 K. Thus, it appears that this induced OO/CO disordering hinders a complete setting of the CE-type antiferromagnetic (AFM) structure characteristic of the $\text{Pr}_{0.5}\text{Ca}_{0.5}\text{MnO}_3$ half-doped manganites. At low T , the higher ac-susceptibility values of $\text{Pr}_{0.5}\text{Ca}_{0.5}\text{Mn}_{0.95}\text{Ga}_{0.05}\text{O}_3$ compared to $\text{Pr}_{0.5}\text{Ca}_{0.5}\text{MnO}_3$ suggests for the former the existence of small FM regions which are embedded in the short-range AFM order matrix. It should be recalled that with the same amount of a magnetic cation, such as chromium, this peak has disappeared and instead a large FM component develops

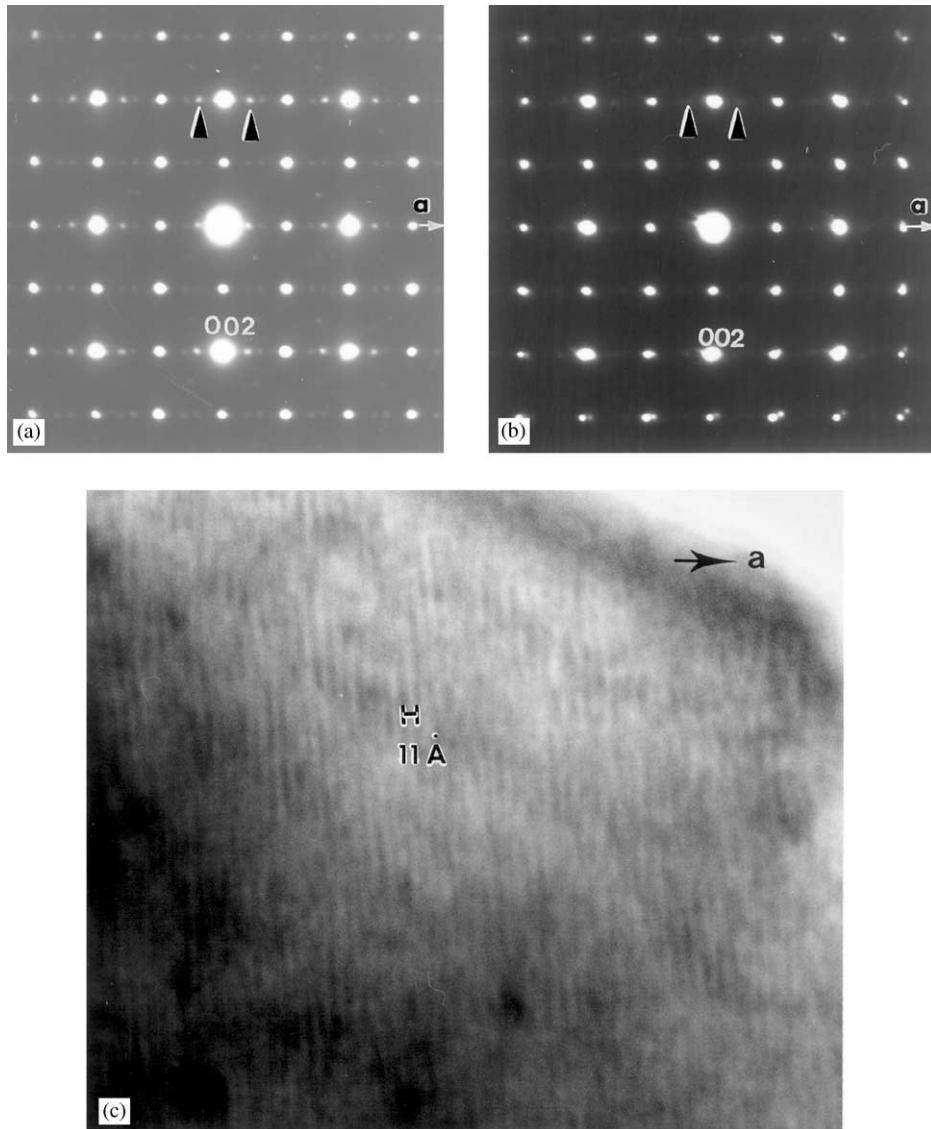


FIG. 2. 92 K [010] electron diffraction patterns of two adjacent areas characterized by clearly (a) and scarcely (b) visible satellites indicated by the arrows. Corresponding lattice image showing a high density of defects in the OO/CO structure (c).

below 150 K (inset of Fig. 1). The latter behavior is in agreement with the much greater ability of Cr to collapse the OO/CO state.

Starting from this disordered “glassy” state for $\text{Pr}_{0.5}\text{Ca}_{0.5}\text{Mn}_{0.95}\text{Ga}_{0.05}\text{O}_3$ in the absence of magnetic field, new features in the measurements of magnetization (M), specific heat (C_p) and resistivity (ρ) are induced under application of an external magnetic field (H) (Fig. 3). At 2.5 K, starting from a virgin state, both $M(H)$ and $C_p(H)$ curves (Fig. 3a and 3b) exhibit four steps as the field increases from 0 to 9 T. However, even in 9 T the magnetization is not saturated since it reaches only $2.7 \mu_B/\text{f.u.}$ instead of $3.5 \mu_B/\text{f.u.}$ Moreover, while the $M(H)$ curve shows only a small remnant magnetization after the cycling, only a slight variation of the specific heat

as the field is returned to 0 (compare both $C_p(H=0)$ values in Fig. 3b) demonstrates the complete irreversibility of this transition. Considering only the existence of jumps in magnetization, one might think of phenomena such as abrupt increases in the spin canting of the majority AFM phase or, alternatively, as sudden reorientation of field-induced FM regions. But the concomitant step steps in the $C_p(H)$ make these assumptions unlikely because these proposed mechanisms are not expected to drastically modify the specific-heat value. Actually, these abrupt steps observed both in $M(H)$ and $C_p(H)$ rather reveal successive, abrupt transformations of AFM regions into FM ones. It should be emphasized that despite the good coincidence in the $C_p(H)$ and $M(H)$ step number, the critical fields values of the steps H_s are shifted up by about 1 T as one goes from

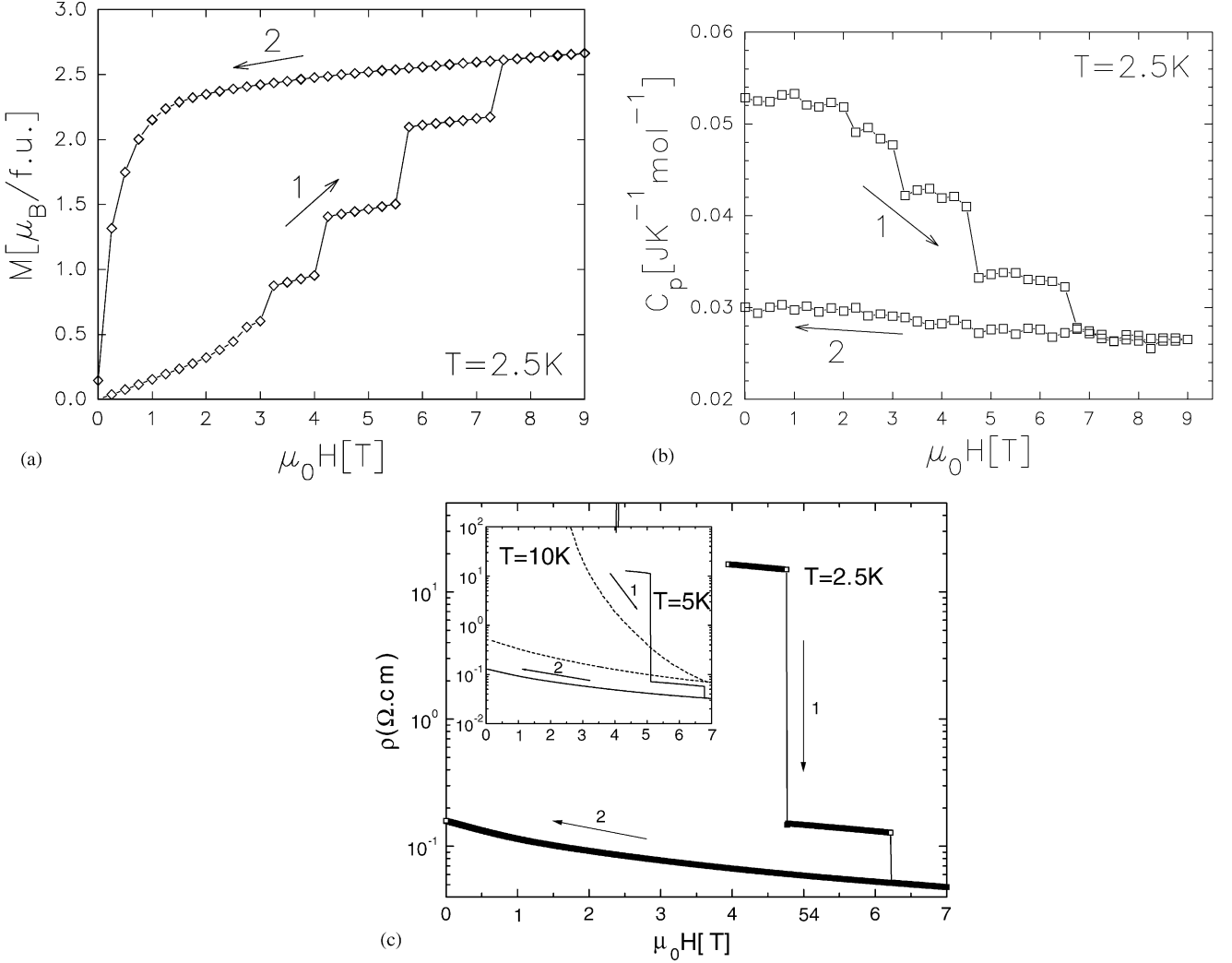


FIG. 3. Physical properties of $\text{Pr}_{0.5}\text{Ca}_{0.5}\text{Mn}_{0.95}\text{Ga}_{0.05}\text{O}_3$ at 2.5 K as a function of the applied magnetic field (H). (a) Magnetization M , (b) specific heat C_p , and (c) resistivity ρ . Inset of 3c: $\rho(H)$ curves of $\text{Pr}_{0.5}\text{Ca}_{0.5}\text{Mn}_{0.95}\text{Ga}_{0.05}\text{O}_3$ at $T=5$ and 10 K. The virgin curve is indicated by the arrow numbered 1 (field increasing branch H_+) and then the field decreasing branch (H_-) is indicated by the arrow 2.

the $C_p(H)$ to the $M(H)$ virgin curves. Steps are also evidenced on the $\rho(H)$ curve registered at 2.5 K. The ρ values for $H=0$ are too high to be measured ($R > 10^7 \Omega$) (Fig. 3c), but, beyond 3.85 T, ρ starts to be measurable. After a first large decrease from $\rho \gg 10^6 \Omega \text{cm}$ to $\sim 10^1 \Omega \text{cm}$ at about 3.85 T, the ρ decrease is not progressive as H increases up to 7 T, but ρ decreases with two abrupt steps at 4.75 and 6.20 T, the first one corresponding to a ρ drop by two orders of magnitude. These H_S values are close to the characteristic field values of the last two steps on the $C(H)$ curve, at 4.5 and 6.5 T, respectively (Fig. 3b). The lack of exact coincidence in the characteristic fields of the steps observed by these various techniques could result first from small natural differences from sample to sample but also from more complex parameters such as the average field rate, number of temperature cycling, etc. A more detailed study of the

history dependence of these steps will be addressed separately (22).

The T dependence of these steps is illustrated by the normalized $C_p(H)/C_p(H=0)$ curves collected at 5 and 10 K in Fig. 4: at 5 K, the virgin curve (increasing field) still exhibits four steps, whereas at 10 K these features have disappeared and are now replaced by a smooth transition. The critical fields of the steps seem to increase as T increases (cf. Figs. 3b and 4). From the $\rho(H)$ curve of Fig. 3c collected for different increasing T and consistently with the $C_p(H)/C_p(H=0)$ at 10 K, the steps have also disappeared at $T=10$ K (this is also true for the $M(H)_{10\text{K}}$ which is not shown).

It must be emphasized that this remarkable effect is not limited to Ga-doped $\text{Pr}_{0.5}\text{Ca}_{0.5}\text{MnO}_3$ manganite, but can be generalized to other nonmagnetic doping elements, with different contents and different electronic structures, as

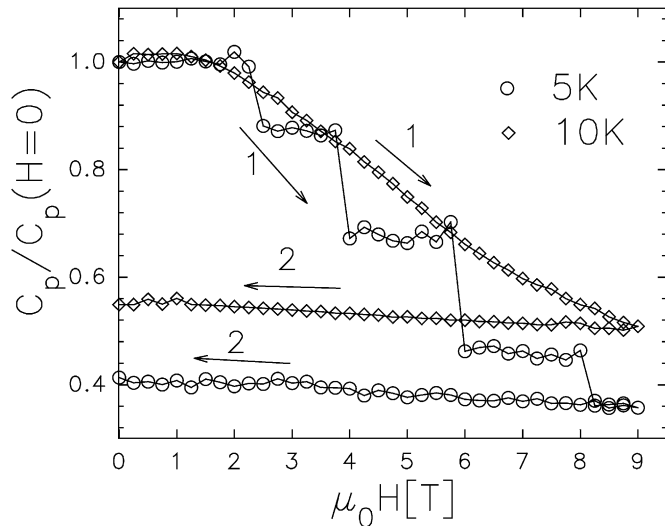


FIG. 4. Normalized specific heat $C_p(H)/C_p(H=0)$ curves of $\text{Pr}_{0.5}\text{Ca}_{0.5}\text{Mn}_{0.95}\text{Ga}_{0.05}\text{O}_3$ at $T=5$ and 10K . 1 and 2 are for the virgin curve (H_+) and H_- branch, respectively.

shown for $\text{Pr}_{0.5}\text{Ca}_{0.5}\text{Mn}_{0.97}\text{Mg}_{0.03}\text{O}_3$ (Fig. 5). In the same way, magnetic cations, are also able to induce such properties, since Co-doped $\text{Pr}_{0.5}\text{Ca}_{0.5}\text{MnO}_3$ manganites are being studied for their similar behavior (23). Thus, it can be stated, that these step-like transitions will be encountered in all $\text{Pr}_{0.5}\text{Ca}_{0.5}\text{MnO}_3$ samples doped with various cations, magnetic or not, provided that they exhibit phase separation at low temperature, i.e., a metastable short-range OO/CO matrix containing small size ferromagnetic domains. In this respect, the doping level of these

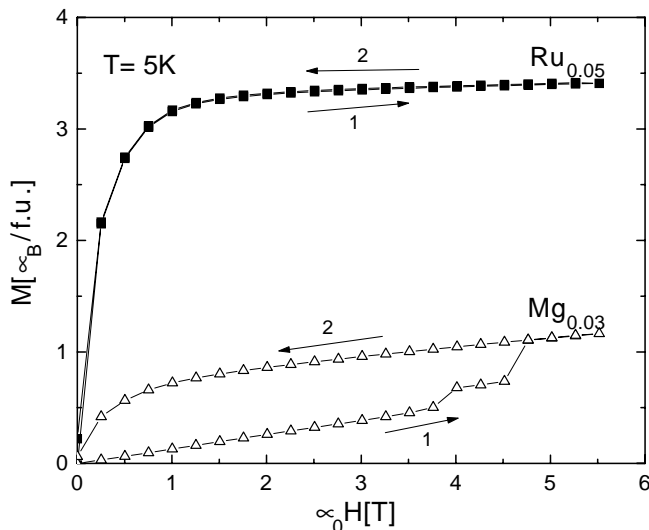


FIG. 5. $T=5\text{K}$; $M(H)$ curves of $\text{Pr}_{0.5}\text{Ca}_{0.5}\text{Mn}_{0.97}\text{Mg}_{0.03}\text{O}_3$ and of $\text{Pr}_{0.5}\text{Ca}_{0.5}\text{Mn}_{0.95}\text{Ru}_{0.05}\text{O}_3$. 1 and 2 are for the virgin curve (H_+) and H_- branch, respectively.

materials will be critical for the appearance of such transitions, since a very high level of magnetic cation may completely suppress the short-range OO/CO matrix. This is confirmed by the absence of step in $\text{Pr}_{0.5}\text{Ca}_{0.5}\text{Mn}_{0.95}\text{Ru}_{0.05}\text{O}_3$ which behaves like a true ferromagnet at 5K saturating at $M_S=3.5\mu_B/\text{f.u.}$ (Fig. 5). These characteristic features are obviously not observed in the case of the pristine compound, in which OO/CO AFM state is very stable and requires a 27T magnetic field to be transformed into an FM, but shows no step in its $M(H)$ curves at any temperature down to 1.4K (12).

Several interpretations of this step-like transitions phenomenon can be proposed. As shown by electron diffraction at 92K , the OO/CO state is only short range (SROO/CO) in these doped manganites and, furthermore, these small regions are characterized by different incommensurable modulation vectors q . At low temperatures ($T < 10\text{K}$), the AFM regions characterized by different q values may undergo steep transitions to FMM (“meta-magnetic” transitions) at different magnetic field values. Note that such a scenario requires that the different q values are discrete rather than being continuously distributed over the sample since, in the latter case, one would expect a broadened AFM–FM transformation. At this point, an electron diffraction study at the temperature of the steps observation is to be performed.

In the literature, such abrupt steps have been reported for the field-dependent magnetization of some ferromagnets [Barkhausen effect (24, 25)], and also in acoustic emission in martensite (26). In the manganites under study, our measurements show an impurity induced-disorder, with the coexistence of several short-range OO/CO-AFM phases and small FM regions with close but different sets of unit cells. This structural phase separation generates strains at the interface regions, as in the martensitic transformation (26). In the case of the Barkhausen effect, the disordered regions and impurities act as pinning centers for the domain walls. The impurities substituted for Mn could also play a similar role in our compounds.

In other respects, dilution by impurities can also induce magnetization jumps in AFM as observed in the case of the site-diluted $\text{Fe}_x\text{Mg}_{1-x}\text{Cl}_2$ (21). For the latter, the distinct magnetization steps are related to avalanches starting from single spin reversal at different lattice sites in the vicinity of the impurities. The substituted cations at the Mn-site in the AFM $\text{Pr}_{0.5}\text{Ca}_{0.5}\text{MnO}_3$ could thus play the same kind of role for the spins flip.

REFERENCES

1. Y. Tokura, Ed., “Colossal Magnetoresistive Oxides.” Gordon and Breach Science, New York, 2000. C. N. R. Rao and B. Raveau, Eds., “Colossal Magnetoresistance, Charge Ordering and other Novel Properties of Manganites.” World Scientific, Singapore, 1998.
2. C. Zener, *Phys. Rev.* **82**, 403 (1951).

3. A. Maignan, Ch. Simon, V. Caignaert, and B. Raveau, *Solid State Commun.* **96**, 62 (1995).
4. H. Y. Hwang, S. W. Cheong, P. G. Radaelli, M. Marezio, and B. Battlog, *Phys. Rev. Lett.* **75**, 914 (1995).
5. P. G. Radaelli, R. M. Ibberson, D. N. Argyriou, H. Casalta, K. H. Andersen, S. W. Cheong, and J. F. Mitchell, *Phys. Rev. B* **63**, 172419 (2001).
6. M. Hervieu, A. Barnabé, C. Martin, A. Maignan, and B. Raveau, *Phys. Rev. B* **60**, R726 (1999).
7. J. B. Goodenough, *Phys. Rev.* **100**, 564 (1955).
8. A. J. Millis, P. B. Littlewood, and B. I. Shraiman, *Phys. Rev. Lett.* **74**, 5144 (1995).
9. A. Asamitsu, Y. Tomioka, H. Kuwahara, and Y. Tokura, *Nature* **388**, 50 (1997).
10. K. Miyano, T. Tanaka, Y. Tomioka, and Y. Tokura, *Phys. Rev. Lett.* **78**, 4257 (1997).
11. V. Kiryukhin, D. Casa, J. P. Hill, B. Keimer, A. Vigliante, Y. Tomioka, and Y. Tokura, *Nature (London)* **386**, 813 (1997).
12. M. Tokunaga, N. Miura, Y. Tomioka, and Y. Tokura, *Phys. Rev. B* **57**, 5259 (1998).
13. B. Raveau, A. Maignan and C. Martin, *J. Solid State Chem.* **130**, 162 (1997); F. Damay, C. Martin, A. Maignan, M. Hervieu, B. Raveau, G. André, and F. Bourée, *Appl. Phys. Lett.* **73**, 3772 (1998).
14. A. Maignan, F. Damay, C. Martin, and B. Raveau, *Mater. Res. Bull.* **32**, 695 (1997).
15. P. V. Vanitha, A. Arulraj, A. R. Raju, C. N. R. Rao, *C. R. Acad. Sci. Paris IIc* **2**, 595 (1999).
16. C. Martin, A. Maignan, M. Hervieu, C. Autret, B. Raveau, and D. I. Khomskii, *Phys. Rev. B* **63**, 174 402 (2001).
17. T. Katsufuji, S. W. Cheong, S. Mori, and C. H. Chen, *J. Phys. Soc. Jpn.* **68**, 1090 (1999).
18. S. Hébert, A. Maignan, R. Frésard, M. Herrieu, R. Retoux, C. Martin, and B. Raveau, *Eur. Phys. J. B* **24**, 85 (2001).
19. T. Kimura, Y. Tomioka, R. Kumai, Y. Okimoto, and Y. Tokura, *Phys. Rev. Lett.* **83**, 3940 (1999).
20. R. Mahendiran, A. Maignan, M. Hervieu, C. Martin, and B. Raveau, *J. Solid State Commun.* **160**, 1 (2001).
21. J. Kushauer, R. van Bentum, W. Kleeman, and D. Bertrand, *Phys. Rev. B* **53**, 11647 (1996).
22. V. Hardy, S. Hébert, C. Martin, A. Maignan, and B. Raveau, to be published.
23. R. Mahendiran *et al.*, to be published.
24. K. A. Dahmen, J. P. Sethna, and O. Perkovic, *IEEE Trans. Magn.* **36**, 3150 (2000).
25. J. J. Becker, *J. Appl. Phys.* **42**, 1537 (1971).
26. E. Vives, J. Ortin, L. Manosa, I. Rafols, R. Perez-Magrane, and A. Planes, *Phys. Rev. Lett.* **72**, 1694 (1994).